

Crystal structures and low-temperature behaviors of the heavy-fermion compounds CeRuGe_3 and $\text{Ce}_3\text{Ru}_4\text{Ge}_{13}$ containing both trivalent and tetravalent cerium

K. Ghosh, S. Ramakrishnan, S. K. Dhar, S. K. Malik, and Girish Chandra
Tata Institute of Fundamental Research, Bombay 400005, India

V. K. Pecharsky and K. A. Gschneidner, Jr.
Ames Laboratory and Department of Materials Science and Engineering, Iowa State University, Ames, Iowa 50011-3020

Z. Hu and W. B. Yelon
University of Missouri Research Reactor, Columbia, Missouri 65211
(Received 27 December 1994; revised manuscript received 20 March 1995)

Two different samples of the Ce-Ru-Ge ternary system of nearly the same composition, $\text{Ce}_3\text{Ru}_4\text{Ge}_{13}$ and CeRuGe_3 , have been studied, as well as the compound $\text{Y}_3\text{Co}_4\text{Ge}_{13}$, which contained a nonmagnetic rare earth as the reference material. Combined x-ray and neutron-diffraction studies of CeRuGe_3 and an x-ray study of $\text{Ce}_3\text{Ru}_4\text{Ge}_{13}$ show that we are dealing with internally distorted (probably 3D modulated) crystals with variable composition, i.e., $\text{Ce}_{4-x}\text{Ru}_4\text{Ge}_{12+x}$ and ranging from at least $x=0$ (1:1:3) to $x=1$ (3:4:13). We have measured the dc magnetic susceptibility, the ac susceptibility, the zero-magnetic-field heat capacity, the magnetic heat capacity in fields ranging from 0 to 9.85 T, and the electrical resistivity. The paramagnetic susceptibility and x-ray crystallography data indicate that the $\text{Ce}_{4-x}\text{Ru}_4\text{Ge}_{12+x}$ alloys contain both trivalent cerium and tetravalent cerium in a 1 to 3 ratio. As far as we are aware, this is the first time such a valence situation has been reported for a cerium compound. In addition, the heat-capacity results show that $\text{Ce}_{4-x}\text{Ru}_4\text{Ge}_{12+x}$ is a heavy fermion with γ varying from 428 to 592 mJ/mol Ce^{3+}K^2 at the 1:1:3 and 3:4:13 compositions, respectively. Zero-field and magnetic-field heat capacity, and ac magnetic susceptibility data suggest that CeRuGe_3 is a spin-glass system below ~ 5 K, which is consistent with the specific features of its crystal structure. $\text{Y}_3\text{Co}_4\text{Ge}_{13}$ displays normal metallic behavior.

I. INTRODUCTION

Numerous studies have been made on the magnetic and superconducting behavior of ternary rare-earth-containing intermetallic compounds with a low content of the rare-earth metal (R), and a transition metal and a nonmetallic or semimetallic element as the second and third components, particularly RMO_6S_8 and RRh_4B_4 .¹ In these compounds superconductivity is due to Mo or Rh clusters, whereas magnetism is due to the lanthanide atoms, and in several compounds both features were found. These discoveries encouraged researchers to look for new materials with similar properties. The synthesis of $\text{R}_3\text{Rh}_4\text{Sn}_{13}$ compounds which have a cubic (space group $Pm\bar{3}n$) structure was reported by Remeika *et al.*² They found that where $R = \text{Sc}, \text{Y}, \text{La}, \text{Yb}, \text{Er}, \text{Tm},$ and Lu the phases are superconducting, whereas magnetic ordering has been observed for $R = \text{Eu}, \text{Gd}, \text{Tb}, \text{Dy}, \text{Ho},$ and Er . The compound $\text{Er}_3\text{Rh}_4\text{Sn}_{13}$ exhibits reentrant superconductivity with $T_s = 0.97$ K and $T_M = 0.57$ K, where T_s is the superconducting transition temperature and T_M is the magnetic ordering temperature. While looking for similar behaviors in germanides, Segre, Braun, and Yvon³ reported the existence of isostructural compounds $\text{R}_3\text{Ru}_4\text{Ge}_{13}$ and $\text{R}_3\text{Os}_4\text{Ge}_{13}$. They have also shown that the corresponding Ru compounds with

$R = \text{Lu}$ and Y undergo a superconducting transition at 2.3 and 1.7 K, respectively, whereas the Ce, Pr, and Er compounds order magnetically at 6.7, 14.2, and 1.2 K, respectively. Simultaneously, they noted that the lattice parameter for the compound $\text{Ce}_3\text{Ru}_4\text{Ge}_{13}$ is smaller than one would expect from the typical unit-cell volume vs atomic number dependence in the lanthanide series (even though the corresponding La compound does not exist). Usually, such a lowering of the unit-cell volume suggests that the Ce atoms exhibit a valence instability and an effective valence between 3+ and 4+ for cerium. If the cerium valence were 4+ then one would not expect valence fluctuations or magnetic order; rather one would expect it to have a nonmagnetic ground state with the compound exhibiting enhanced Pauli paramagnetism.

Crystal structures of these series of cubic compounds with a composition close to RMX_3 , where R is a rare-earth metal, M a transition metal, and X is Ge or Sn, have been investigated for several different M representatives. As already mentioned, Remeika *et al.*² have reported a cubic structure with a primitive unit cell ($a \approx 9.7$ Å) for the $\text{R}_3\text{Rh}_4\text{Sn}_{13}$ series. They also found some stannides with a face-centered-cubic unit cell, and others which are probably tetragonal. Later Hodeau *et al.*⁴ reported another type of possible distortion leading to a body-centered-cubic unit cell with a unit-cell volume eight times larger. Eisenmann and Schäfer⁵ give

the details of crystal structure of the compounds $RRuSn_3$, which are characterized by the same primitive cubic unit cell as reported for $R_3Rh_4Sn_{13}$,² but have a different distribution of rare-earth and tin atoms in the unit cell which slightly shifts the composition from 3:4:13 to 1:1:3. As far as we know, there are two reports on the crystal structure of germanides: Segre, Braun, and Yvon³ and Bruskov, Pecharsky, and Bodak⁶ reported details on the crystal structures of $Y_3Ru_4Ge_{13}$ and $Y_3Co_4Ge_{13}$, respectively. Both compounds were found to crystallize in the space group $Pm\bar{3}n$ with lattice parameter close to 9 Å. Segre, Braun, and Yvon³ reported an ordered crystal structure for $Y_3Ru_4Ge_{13}$, but mentioned that they observed enormously large values of the displacement (thermal) parameters for both independent germanium sites [2(*a*) and 24(*k*)]. Bruskov, Pecharsky, and Bodak⁶ proposed a disordered variant of the crystal structure where germanium atoms partially occupy two different 24(*k*) sites. Both papers agree that neither the ordered nor the disordered structure models describe the compound's exact crystal structure, and that these models represent some sort of an "average" structure with an accuracy which could be reached by using classical three-dimensional diffraction theory.

Thus the series of cubic (or pseudocubic) ternary intermetallic compounds, containing germanium and/or tin, still maintain a strong interest for solid-state physics and chemistry. This paper presents our results on the room-temperature crystal structure and the low-temperature properties of the compound earlier referred to as " $Ce_3Ru_4Ge_{13}$."

II. EXPERIMENTAL DETAILS

Three samples having the chemical compositions of $Ce_3Ru_4Ge_{13}$ (sample no. 1), $CeRuGe_3$ (sample no. 2), and $Y_3Co_4Ge_{13}$ were prepared by arc-melting the individual constituents. The arc melting was carried out under high-purity argon at normal pressure. The $Ce_3Ru_4Ge_{13}$ (sample no. 1) was prepared at the Tata Institute of Fundamental Research, using commercially available cerium, ruthenium, and germanium with a certified purity of 99.9, 99.99, and 99.99 wt %, respectively. Cerium and yttrium, used in synthesis of $CeRuGe_3$ (sample no. 2) and $Y_3Co_4Ge_{13}$, were prepared at the Ames Laboratory's Materials Preparation Center and were >99.9 at. % pure. Cobalt, ruthenium, and germanium were purchased from commercial sources and were certified to be 99.99+ wt % pure. All three samples were arc melted up to seven times each to ensure the sample's homogeneity and then annealed at 900°C for two weeks in helium-filled quartz tubes. All specimens were checked for the presence of second phases using x-ray diffraction, and were single phase within the accuracy of the method. The diffraction patterns of both as-cast $CeRuGe_3$ and $Y_3Co_4Ge_{13}$ were found to contain a significant number of diffraction maxima due to a second, and possibly a third, unidentified impurity phase(s). However, after the above-noted heat treatment all of the extra peaks were no longer observed in the x-ray patterns. The measurements on cerium-containing samples were performed indepen-

dently, as described below.

$Ce_3Ru_4Ge_{13}$. The temperature dependence of dc susceptibility was measured using a superconducting quantum interference device (SQUID) magnetometer (Quantum Design) in a field of 5 kOe in the temperature range from 4 to 300 K. The ac susceptibility was measured using a home-built susceptometer⁷ from 1.5 to 5 K. The resistivity was measured using a four-probe dc technique with contacts made using an ultrasonic soldering iron with nonsuperconducting solder on a cylindrical sample 2 mm in diameter and 10 mm in length. The temperature was measured using a calibrated Si diode sensor (Lake Shore Inc.). The sample voltage was measured with a Keithley nanovoltmeter with a current of 25 mA using a 20 ppm stable Hewlett-Packard (HP) current source. All the data were collected using an IBM-compatible PC/AT via an IEEE-488 interface. The heat capacity in zero field between 2 and 20 K was measured using an automated semiadiabatic heat-pulse method. A calibrated Ge-resistance thermometer (Lake Shore Inc.) was used as the temperature sensor in this range.

$CeRuGe_3$. The zero- and high-magnetic-field (0–9.85 T) heat capacity from ~1.5 to ~20 K was measured using an adiabatic heat-pulse-type calorimeter.⁸ The dc susceptibility was measured using a Faraday balance from 1.5 to 285 K in fields ranging from ~0.5 to ~1.9 T. The ac susceptibility and dc magnetization were measured using an ac/dc susceptometer/magnetometer (Lake Shore, model no. 7225).

X-ray-diffraction studies were performed using data obtained from a SCINTAG automated powder diffractometer with monochromated Cu K_α radiation. Neutron-powder-diffraction data were obtained using a monochromated neutron beam (Missouri Research Reactor, $\lambda=1.4783$ Å) from a cylindrically shaped powdered sample. All crystallographic calculations, including full-profile refinement of atomic parameters from both x-ray and neutron-diffraction data, were performed using the program system⁹ CSD and a 486/87-based PC.

III. RESULTS

A. Crystal structure and composition

Since there are contradictory reports on the composition of Sn-based and the crystal structure of Ge- and Sn-based compounds with a primitive cubic crystal structure (space group $Pm\bar{3}n$, $a=9-9.5$ Å, see the Introduction above), we have tried to clarify the situation using power-diffraction data. (Most of the previous x-ray work was done on single crystals.) First of all, we would like to stress that both the x-ray and neutron-diffraction patterns of $CeRuGe_3$ never showed any evidence of reflections which required the unit cell to be changed from primitive cubic to any other cubic (face or body centered) or to a tetragonal one. Therefore we tried to refine several different models of crystal structure using a basic primitive cubic unit cell and space group $Pm\bar{3}n$. We find that both the ordered (suggested by Segre, Braun, and Yvon³) and disordered (suggested by Bruskov, Pecharsky, and Bodak⁶) structure models give approximately the same fit

results. The ordered-structure least-squares fit (Table I) is characterized by an extremely large displacement-parameter anisotropy for the atoms in $2(a)$ (Ce2) and $24(k)$ (Ge) sites. The “abnormality” is obvious also from the electron density distribution maps, which are shown in Fig. 1. This figure represents the sections of the electron density distribution in the planes parallel to the ab plane, calculated for a square with a 2 \AA edge, and with an atom located at the center of each plane (i.e., every atom has the relative coordinates of $x=0$ and $y=0$, and the corners of the squares have the relative coordinates of $1, 1; 1, -1; -1, 1$; and $-1, -1$, respectively). The Ce1 [Fig. 1(a)] and Ru [Fig. 1(c)] atoms are characterized by a normal, round electron density distribution. The Ce2 atom [Fig. 1(b)] has the electron density maximum shifted off center (i.e., off the ideal crystallographic position) by approximately 0.5 \AA along the crystallographic axes, while the Ge atom [Fig. 1(d)] electron density is strongly elongated toward the corners of the square. Simultaneously, one can observe a significant reduction in the magnitude of electron density for Ce2 and Ge atoms, compared to what is expected from the number of electrons for Ce, Ru, and Ge. These features of the electron density distribution allow us to build another, slightly distorted model of the CeRuGe_3 crystal structure. The disordered structure model can be constructed when one moves the Ce2 and Ge atoms away from their ideal crystallographic positions [i.e., the atom from the $2(a)$ site is shifted out of the center of symmetry, and the atoms from the $24(k)$ site have been split into two $24(k)$ sites with partial occupancies and similar positional parameters] as was done by Bruskov, Pecharsky, and Bodak⁶ to eliminate the unusual anisotropy of the appropriate Ge atom. After such a distortion, the least-squares fitting of the calculated powder-diffraction pattern to the observed data was satisfactory and the displacement (thermal) parameters were close to normal. The resulting distortion therefore is as follows:

$$2 \text{ Ce2 in } 12(f): x, 0, 0; x = 0.06$$

[instead of Ce2 in $2(a)$: $0, 0, 0$] and $\sim 12 \text{ Ge 1 in } 24(k)$:

$$x, y, 0; x = \sim 0.34, y = \sim 0.16,$$

and

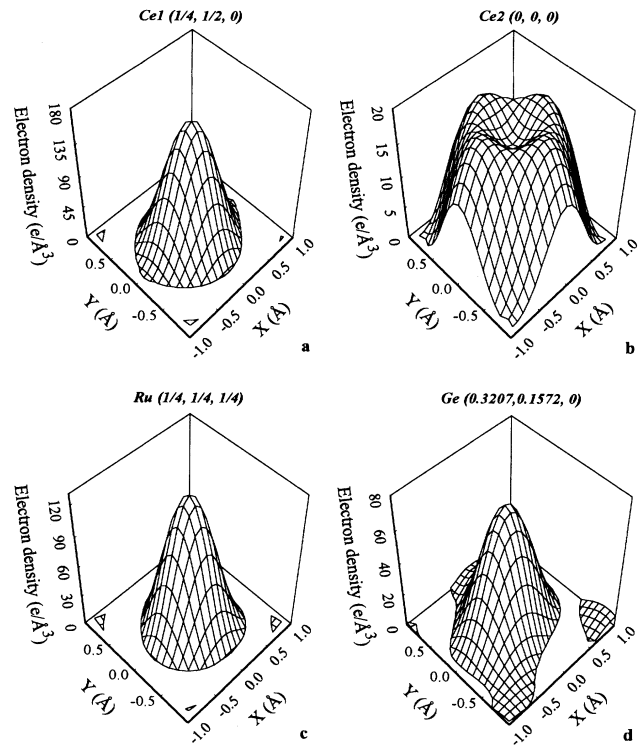


FIG. 1. The electron density distribution around all of the atoms in the four different positional sites of the compound CeRuGe_3 : (a) Ce1, (b) Ce2, (c) Ru, and (d) Ge.

$$\sim 12 \text{ Ge2 in } 24(k): x, y, 0; x = \sim 0.29, y = \sim 0.14$$

[instead of $24 \text{ Ge in } 24(k)$: $x, y, 0; x = \sim 0.32, y = \sim 0.15$]. The observed and calculated (ordered model) x-ray and neutron-diffraction data for CeRuGe_3 are shown in Fig. 2.

Since we have used both x-ray and neutron-diffraction data, this allowed us to determine which type of atoms occupy the $2(a)$ site position (cerium has the largest atomic scattering factor for x rays, and germanium the

TABLE I. Atomic parameters for CeRuGe_3 (sample no. 2), space group $Pm\bar{3}n$, $a = 9.0061(4) \text{ \AA}$. Neutron-diffraction data results are shown in bold italics. The final residuals are as follows: $R_I = 0.052$ (x-ray-diffraction data, 99 possible reflections) and $R_I = 0.065$ (neutron-diffraction data, 102 possible reflections), $R_I = \sum(|I_{\text{obs}} - I_{\text{cal}}|) / \sum(I_{\text{obs}})$.

Atom	x/a	y/b	z/c	$B_{\text{eq}} (\text{\AA}^2)$	B_{11}^a	B_{22}	B_{33}	B_{12}	B_{13}	B_{23}
Ce1 in $6(d)$	$1/4$	$1/2$	0	0.4(1)	0.5(2)	0.3(1)	B_{22}	0	0	0
	<i>$1/4$</i>	<i>$1/2$</i>	<i>0</i>	<i>0.4(2)</i>	<i>0.5(3)</i>	<i>0.3(2)</i>	<i>B_{22}</i>	<i>0</i>	<i>0</i>	<i>0</i>
Ce2 in $2(a)$	0	0	0	16(1)	16(1)	B_{11}	B_{11}	0	0	0
	<i>0</i>	<i>0</i>	<i>0</i>	<i>14(2)</i>	<i>14(2)</i>	<i>B_{11}</i>	<i>B_{11}</i>	<i>0</i>	<i>0</i>	<i>0</i>
Ru in $8(e)$	$1/4$	$1/4$	$1/4$	0.2(1)	0.2(1)	B_{11}	B_{11}	0.1(1)	B_{12}	B_{12}
	<i>$1/4$</i>	<i>$1/4$</i>	<i>$1/4$</i>	<i>1.1(1)</i>	<i>0.9(1)</i>	<i>B_{11}</i>	<i>B_{11}</i>	<i>0.4(1)</i>	<i>B_{12}</i>	<i>B_{12}</i>
Ge in $24(k)$	0.3223(5)	0.1577(5)	0	1.9(2)	4.1(3)	1.5(2)	0.1(2)	2.0(2)	0	0
	<i>0.3207(5)</i>	<i>0.1572(4)</i>	<i>0</i>	<i>2.5(2)</i>	<i>4.5(2)</i>	<i>2.0(2)</i>	<i>0.5(2)</i>	<i>2.0(1)</i>	<i>0</i>	<i>0</i>

^aDisplacement parameters are presented in \AA^2 ($B_{ij} = 8\pi^2 u_{ij}^2$); $B_{\text{eq}} = 1/3[B_{11}a^2 + \dots + 2B_{23}b^*c^*bc \cos(\alpha)]$.

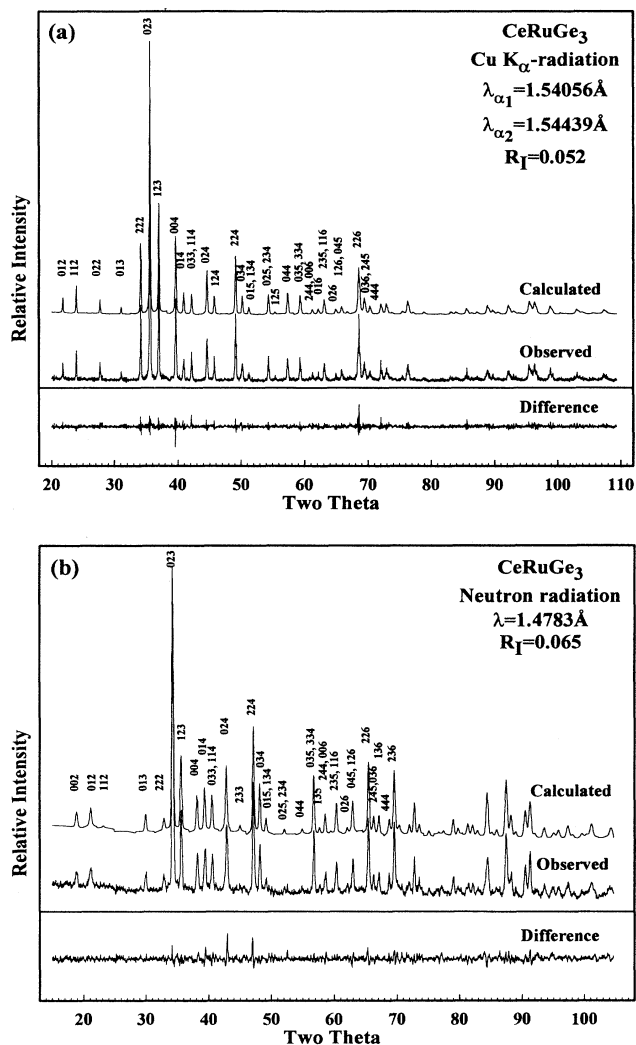


FIG. 2. Comparison of the observed and calculated x-ray (a) and neutron (b) powder-diffraction data of CeRuGe_3 . All the data are shown at the same scale.

lowest one; while cerium has the lowest scattering amplitudes for neutrons and germanium the highest). When germanium atoms were placed in the $2(a)$ position, the displacement parameters were quite different ($\sim 6 \text{ \AA}^2$ for x rays and $\sim 25 \text{ \AA}^2$ for neutron-diffraction data). Usually, one expects all the least-squares parameters, including displacement ones, to be the same within the estimated standard deviation value, because the exact same material was examined by x rays and neutrons. As one can see from Table I, when cerium is placed in the $2(a)$ position both x-ray and neutron-diffraction data give essentially the same positional and displacement parameters for *all* of the atoms independent of the diffraction method.

Analysis of the displacement parameters (i.e., the B values listed in Table I) and the electron density maps [Figs. 1(b) and 1(d)] showed that the Ce2 and all of the germanium atoms in the CeRuGe_3 crystal structure show some kind of internal disorder. In general, such highly

anisotropic thermal vibrations are not observed in intermetallic compounds. This result agrees with the observation of Segre, Braun, and Yvon,³ who noted that the Ge1 and Ge2 atoms, which occupy the $2(a)$ and the $24(k)$ positions, respectively, in the $\text{Y}_3\text{Ru}_4\text{Ge}_{13}$ structure, have large thermal parameters. These authors did not mention whether or not they tried to refine the displacement-parameter anisotropy, but they noted that their electron density maps show that Ge1 has the shape of a jack with its prongs aligned along unit-cell axes, and that Ge2 has the form of an elongated disk. Their results are in excellent agreement with our electron density distribution maps (see Fig. 1) and with anisotropic thermal parameters found for Ce1 and Ge atoms in the structure of CeRuGe_3 (Table I). The structural model given by Bruskov, Pecharsky, and Bodak⁶ for the compound $\text{Y}_3\text{Co}_4\text{Ge}_{13}$ has two sets of $24(k)$ positions occupied by 24 germanium atoms. Again the difference between the positional parameters supports an elongated disklike shape of germanium. However, in contrast to the structures of CeRuGe_3 and $\text{Y}_3\text{Ru}_4\text{Ge}_{13}$, the enhancement of the thermal parameter of the Ge atom, which occupies the $2(a)$ position in the compound $\text{Y}_3\text{Co}_4\text{Ge}_{13}$, is not so obvious. Eisenmann and Schäfer⁵ found a similar situation with the crystal structure of LaRuSn_3 . They note that the lanthanum atoms which occupy the $2(a)$ positions have a greatly enhanced thermal parameter and the tin atom in the $24(k)$ position is strongly anisotropic and has the elongated disk form. Therefore our observations are consistent with prior observations of similar structurally related compounds. Thus it is reasonable to assume that we are dealing with a series of two- or three-dimensionally modulated structures, but more detailed crystallographic work is required.

Finally, we would like to note that our cerium samples (nos. 1 and 2) were initially synthesized at different starting compositions ($\text{Ce}_3\text{Ru}_4\text{Ge}_{13}$ and CeRuGe_3 , respectively). X-ray and neutron-diffraction analysis confirmed the composition for the sample no. 2. The quality of the x-ray-diffraction pattern for sample no. 1 was not sufficiently satisfactory to make a definite conclusion about the sample's composition, but the value of the lattice parameter is lower than that for sample no. 2: a least-squares unit-cell parameter refinement gives $a = 9.0494(4) \text{ \AA}$ for sample no. 1 ($\text{Ce}_3\text{Ru}_4\text{Ge}_{13} \equiv \text{Ce}_{0.75}\text{RuGe}_{3.25}$) and $a = 9.0661(4) \text{ \AA}$ for sample no. 2 (CeRuGe_3). The same value, close to 9.04 \AA , is given by Segre, Braun, and Yvon³ for their $\text{Ce}_3\text{Ru}_4\text{Ge}_{13}$ sample (as estimated from a plot of the unit-cell parameter vs atomic number). All this makes it quite reasonable to conclude that all three samples (the two samples we are working with, and the sample mentioned by Segre, Braun, and Yvon³) are actually the same compound which has a variable composition, extending from the 1:1:3 to the 3:4:13 stoichiometry. The only difference between these two terminal compositions is due to variation of the rare-earth and germanium contents: the 1:1:3 composition is characterized by 20% rare earth and 60% germanium (all percentages are atomic), while the 3:4:13 composition has 15% rare earth and 65% germanium. The amount of

the transition metal (Ru) remains the same—20 at. %. Therefore the unit-cell reduction which takes place when going from CeRuGe_3 to $\text{Ce}_3\text{Ru}_4\text{Ge}_{13}$ is consistent with decreasing the amount of the largest-atomic-size component (Ce) and, most likely, a germanium substitution for cerium in both the $2(a)$ and $6(d)$ positions to form the CeRuGe_3 - $\text{Ce}_3\text{Ru}_4\text{Ge}_{13}$ continuous solid solution, i.e., $\text{Ce}_{4-x}\text{Ru}_4\text{Ge}_{12+x}$. A substitution in the $2(a)$ site is not prohibited by crystal chemistry, because the atom(s) located at the $2(a)$ position has (have) an icosahedral arrangement which is large enough to contain either the smaller germanium or the larger cerium (see the list of interatomic distances for CeRuGe_3 given in the Table II). Substitution of germanium in the $6(d)$ position is no problem either, since the size of the Ce atom (which is tetravalent—see below) is only somewhat larger than that of the germanium atom, 1.672 vs 1.378 Å, respectively. Therefore the $\text{Ce}_3\text{Ru}_4\text{Ge}_{13}$ sample has the possibility of about a 25% substitution of germanium atoms for cerium atoms in the two sublattices. The germanium distribution in the two cerium sublattices will be discussed in the next section on the magnetic susceptibility results. Sample no. 2 (CeRuGe_3), however, is characterized by the presence of two independent cerium sublattices: one of which, holding the majority of cerium atoms, $6(d)$, is ordered, while the second $2(a)$ seems to be distorted—affected by two-dimensional (2D) or 3D displacement modulations. The ruthenium sublattice, $8(e)$, for both samples is ordered too, and germanium sublattice(s), $24(k)$, are distorted (probably 2D or 3D modulated) for both of our samples.

B. dc susceptibility and electrical resistivity studies

The temperature dependence of the inverse dc susceptibility is shown on Fig. 3(a) with the inset clarifying the

TABLE II. Interatomic distances for the compound CeRuGe_3 .

Atoms		Distance (Å) from x-ray data	Distance (Å) from neutron data
Ce1	8 Ge	3.127(3)	3.132(3)
	4 Ge	3.172(5)	3.173(4)
	4 Ru1	3.205(1)	3.205(1)
	2 Ce1	4.533(1)	4.544(1)
	4 Ce2	5.068(1)	5.079(1)
Ce2	12 Ge	3.253(5)	3.238(4)
	12 Ce1	5.068(1)	5.079(1)
	8 Ce2	7.851(1)	7.869(1)
Ru	6 Ge	2.503(2)	2.501(2)
	3 Ce1	3.205(1)	3.205(1)
Ge	2 Ru	2.503(2)	2.501(2)
	2 Ge	2.827(6)	2.848(5)
	1 Ge	2.859(7)	2.851(6)
	2 Ce1	3.127(3)	3.132(3)
	1 Ce1	3.172(5)	3.173(4)
	1 Ce2	3.253(5)	3.238(4)

low-temperature behavior. It is obvious that both sets of data (from samples no. 1 and no. 2) show an anomaly around 7 K, which is consistent with the magnetic transition temperature reported by Segre, Braun, and Yvon.³ However, our heat-capacity measurements, which are discussed below, clearly rule out a bulk nature of this

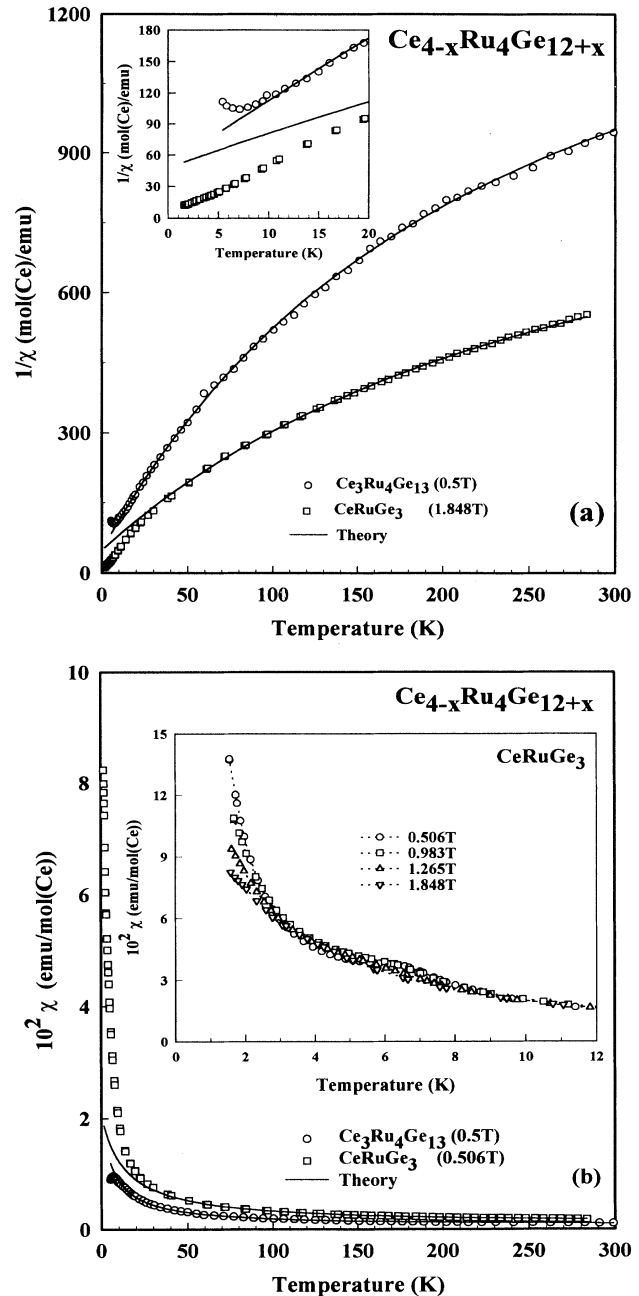


FIG. 3. (a) Inverse molar dc susceptibilities of CeRuGe_3 (sample 2) and $\text{Ce}_3\text{Ru}_4\text{Ge}_{13}$ (sample 1) and the least-squares fit results. The inset shows the low-temperature details. (b) The dc susceptibilities are shown together with least-squares fit results. The inset shows the field dependence of the dc susceptibility at low temperature.

“magnetic transition.” Neither sample obeys the simple Curie-Weiss law

$$\chi = N\mu_{\text{eff}}^2/3k_B(T - \theta_p), \quad (1)$$

but they could be fitted to a modified Curie-Weiss law, which is suitable for materials displaying valence-fluctuating behavior or having a large temperature-independent susceptibility:

$$\chi = N\mu_{\text{eff}}^2/3k_B(T - \theta_p) + \chi_0, \quad (2)$$

where χ_0 represents the temperature-independent part of the magnetic susceptibility, including the core-electron diamagnetism and the Pauli paramagnetism and Van Vleck terms.

The $\text{Ce}_3\text{Ru}_4\text{Ge}_{13}$ sample obeys the modified Curie-Weiss law from room temperature down to ~ 8 K, i.e., down to the temperature where the 7 K anomaly appears; see Table III for the values of the fit parameters. The calculated effective magnetic moment $[(1.06 \pm 0.01)\mu_B$ per Ce atom] is much lower than one would expect for a free Ce^{3+} ion ($2.54\mu_B$), and the paramagnetic Curie temperature (θ_p) is slightly negative (-7.0 ± 0.2 K). The CeRuGe_3 sample obeys the same law [Eq. (2)] down to about 50 K, and then the inverse susceptibility shows negative deviation, which is suggestive of a tendency toward ferromagnetic (or ferrimagnetic) magnetic ordering. The effective magnetic moment for this sample is somewhat higher $[(1.23 \pm 0.01)\mu_B$ per Ce atom], and the paramagnetic Curie temperature is about the same as for the former sample (-7.5 ± 0.2 K). These results might suggest that the effective cerium valence is higher than $3+$, and cerium displays valence-fluctuation behavior. Although the effective paramagnetic moment is rather low, the overall magnetic susceptibility behavior is more like that of a cerium system which is largely trivalent rather than one which is mixed valent [e.g., compare the susceptibility curves of CeNiGe_2 or CeNiSn_2 (Fig. 6 of Ref. 10) in which Ce is $3+$ with that of CeNiSi_2 (Fig. 4 of Ref. 10) in which Ce is mixed valent]. The situation for CeRuGe_3 may be explained if the cerium atoms in the two different sites have different valences, i.e., in particular the Ce1 atoms in the $6(d)$ sites are tetravalent and exhibit Pauli paramagnetism, while the Ce2 atoms in the $2(a)$ sites are trivalent and exhibit Curie-Weiss behavior. In such a case, the effective magnetic moment is given by

$$p_{\text{eff}} = [(2/8)(2.54)^2 + (6/8)(0)^2]^{1/2}, \quad (3)$$

which yields a $p_{\text{eff}} = 1.27\mu_B$ for CeRuGe_3 , which compares well with the experimental value of $1.23\mu_B$.

TABLE III. Paramagnetic properties of $\text{Ce}_3\text{Ru}_4\text{Ge}_{13}$ and CeRuGe_3 .

Property	$\text{Ce}_3\text{Ru}_4\text{Ge}_{13}$ (sample no. 1)	CeRuGe_3 (sample no. 2)
$\mu_{\text{eff}}/\text{Ce}$ (μ_B)	1.06(1)	1.23(1)
θ_p (K)	-7.0(2)	-7.5(4)
χ_0 (emu/mol Ce)	$6.0(1) \times 10^{-2}$	$7.8(1) \times 10^{-2}$

The situation is a little more complicated for $\text{Ce}_3\text{Ru}_4\text{Ge}_{13}$. If all the germanium atoms which substitute for Ce (25% for the 3:4:13 composition) occupy the Ce^{3+} sites then the material should have an effective magnetic moment of zero and the temperature dependence of the magnetic susceptibility should be essentially constant, i.e., that of an enhanced Pauli paramagnet, since there would be only tetravalent Ce atoms in the $6(d)$ positions and no trivalent Ce atoms in the $2(a)$ positions. But since there is an observed effective magnetic moment ($p_{\text{eff}} = 1.06\mu_B$), this eliminates this possibility. On the other hand, if the germanium atoms substitute for just cerium atoms in the $6(d)$ positions then $\text{Ce}_3\text{Ru}_4\text{Ge}_{13}$ would have two Ce^{3+} and four Ce^{4+} atoms, and one would expect a p_{eff} value of $1.47\mu_B$, i.e., the first term of Eq. (3) would be $(2/6)(2.54)^2$. Since the theoretical value is too large compared with the observed value, this cannot be the correct distribution of germanium atoms on the cerium sites. A reasonable answer, consistent with experiment, would be given by an equal substitution of germanium for the cerium over the two sites, i.e., 25% of the $2(a)$ and also the $6(d)$ sites are occupied by germanium atoms. That is, there are 1.5 Ce + 0.5 Ge atoms in the $2(a)$ positions and 4.5 Ce + 1.5 Ge atoms in the $6(d)$ positions. This distribution of cerium and germanium atoms among the two sites is also consistent with the electronic specific heat constants γ derived for the two compositions; see below in the next section. Furthermore, the observation of a large γ for $\text{Ce}_3\text{Ru}_4\text{Ge}_{13}$ definitely rules out the first possibility noted above. Thus for $\text{Ce}_3\text{Ru}_4\text{Ge}_{13}$ the first term on the right-hand side of Eq. (3) becomes $(0.75)(2/8)(2.54)^2$, and this yields a theoretical value of $p_{\text{eff}} = 1.10\mu_B$, which is also in good agreement with the observed value of $1.06\mu_B$.

The existence of both trivalent and tetravalent cerium in the $\text{Ce}_{4-x}\text{Ru}_4\text{Ge}_{12+x}$ system is also confirmed by the bond lengths calculated from the x-ray crystallographic data; see Table II. The shortest Ce1-Ge bond length is 3.127 Å, while that between Ce2 and Ge is 3.253 Å, i.e., a difference of 0.126 Å. This difference is consistent with, but somewhat smaller than, the difference between the metallic radii of hypothetical Ce^{3+} (1.846 Å) and hypothetical Ce^{4+} (1.672 Å), 0.174 Å (for comparison the radii of γ -Ce and α -Ce are 1.824 and 1.73 Å, respectively).¹¹

Thus from the paramagnetic susceptibility and x-ray crystallography data we conclude that the $\text{Ce}_{4-x}\text{Ru}_4\text{Ge}_{12+x}$ alloys contain both trivalent cerium and tetravalent cerium in a 1:3 ratio.

Although the negative Curie temperature is evidence that the compound may have an antiferromagnetic ground state, a high magnetic field > 1.5 T destroys the ~ 7 K anomaly [Fig. 3(b), inset], which is again typical, at least for ferromagnetic systems. We believe that the ~ 7 K anomaly is due to the presence of a small amount of a second phase (see the following section for details) in both of our samples. Even though x-ray-diffraction studies revealed that the samples are pure, the usual sensitivity of this method does not allow one to detect less than 5–7% of the presence of a second phase. The strong up-

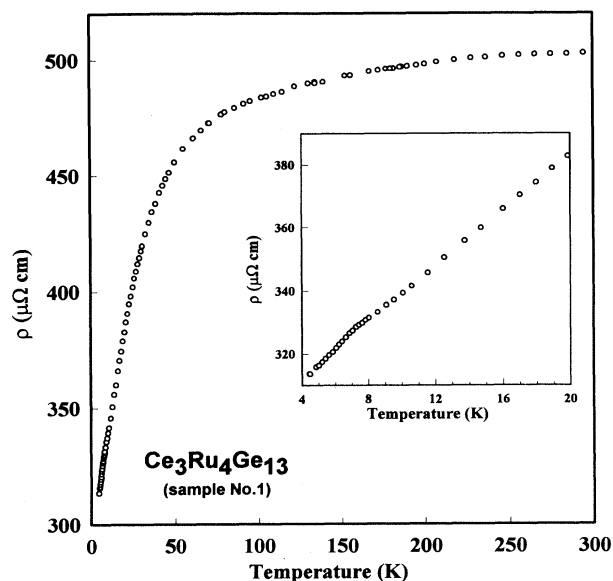


FIG. 4. The electrical resistivity of $\text{Ce}_3\text{Ru}_4\text{Ge}_{13}$. The inset shows the low-temperature details.

turn of the χ vs T dependence and the χ field dependence [inset of Fig. 3(b)] (at least for CeRuGe_3) are suggestive of ferromagnetic ordering.

Figure 4 illustrates the ρ vs T dependence for $\text{Ce}_3\text{Ru}_4\text{Ge}_{13}$. The small change of slope around 7 K again is evident and is consistent with the magnetic susceptibility results (see above) and the heat-capacity data (see below). The resistivity above 50 K is large, and exhibits an unusual temperature dependence compared to that of normal Ce^{3+} -based compounds. The temperature dependence of the resistivity as well as that of the magnetic susceptibility are similar to those of UPt_3 (see Ref. 12).

C. Heat capacity, ac susceptibility, and magnetization

Figure 5 displays the zero-magnetic-field heat capacity of cerium-containing samples no. 1 and no. 2, together with the heat capacity of $\text{Y}_3\text{Co}_4\text{Ge}_{13}$, while Fig. 6 shows the high-magnetic-field heat capacity of CeRuGe_3 . It is obvious that the heat capacities of the two cerium samples are much closer to one another than the dc susceptibilities [see Fig. 3(a) above]. Both $\text{Ce}_{4-x}\text{Ru}_4\text{Ge}_{12+x}$ samples have a small anomaly around 6.5–6.8 K and an upturn at the lowest temperature. The upturn is much more visible for CeRuGe_3 . Unfortunately, the $\text{La}_{4-x}\text{Ru}_4\text{Ge}_{12+x}$ compound does not exist and thus we are unable to subtract off lattice contribution from the measured heat capacity of the cerium alloys in order to determine the other contributions to the heat capacity of $\text{Ce}_{4-x}\text{Ru}_4\text{Ge}_{12+x}$. But, since the $\text{Y}_3\text{Co}_4\text{Ge}_{13}$ compound is isostructural with $\text{Ce}_3\text{Ru}_4\text{Ge}_{13}$, we measured the heat capacity of the yttrium compound to help evaluate the various contributions to the heat capacity of $\text{Ce}_3\text{Ru}_4\text{Ge}_{13}$ and CeRuGe_3 . The heat capacity of $\text{Y}_3\text{Co}_4\text{Ge}_{13}$ is quite

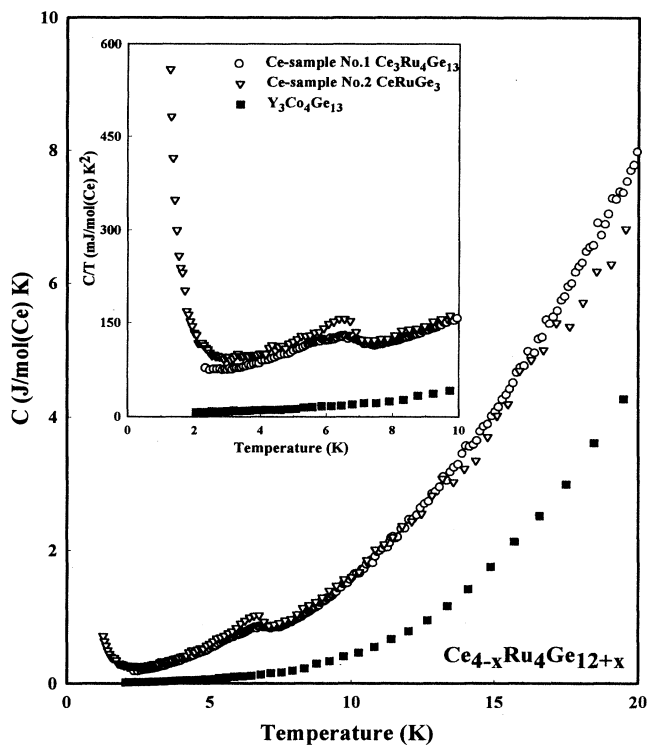


FIG. 5. The zero-magnetic-field heat capacity of CeRuGe_3 (sample 2), $\text{Ce}_3\text{Ru}_4\text{Ge}_{13}$ (sample 1), and $\text{Y}_3\text{Co}_4\text{Ge}_{13}$ between ~ 1.5 and 20 K. The inset shows the heat capacity between ~ 1.5 and 10 K.

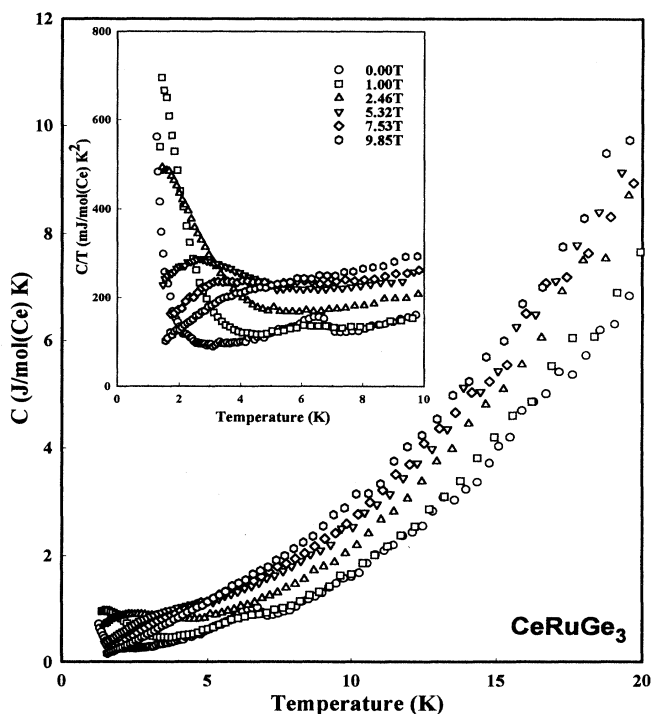


FIG. 6. The magnetic-field heat capacity of CeRuGe_3 (sample 2) from ~ 1.5 to 20 K. The inset shows the C/T vs T plots from ~ 1.5 and 10 K.

normal, showing no anomalies down to $T=2$ K. Below $T=9$ K the heat capacity of $Y_3Co_4Ge_{13}$ could be fitted to the equation

$$C = \gamma T + \beta T^3, \quad (4)$$

which gives the electronic specific heat coefficient $\gamma = 5.7(1)$ mJ/(mol Y) K² and the Debye temperature $\Theta_D = 354(34)$ K. The heat-capacity behavior of both Ce-containing samples seems to show a linear region between ~ 3 and ~ 6 K in a C/T vs T^2 plot. Fitting the data in this region to Eq. (4) yields a " Θ_D " of 187(7) K for $Ce_3Ru_4Ge_{13}$. But when one compares this value with that for the $Y_3Co_4Ge_{13}$ compound, assuming that $\Theta_D \propto M^{-1/2}$ (where M is the molecular weight per formula unit), the observed Θ_D value for the cerium compound is too low by a factor of ~ 1.7 . This suggests that any Θ_D and γ values that might be estimated from the heat capacity between 3 and 6 K using Eq. (4) for the two cerium compounds are not realistic.

One can, however, use the heat-capacity data above the 7 K heat-capacity bump to determine the electronic contribution to the heat capacity by subtracting off the appropriate lattice contribution. This can be done by using the heat-capacity results obtained on $Y_3Co_4Ge_{13}$ by correcting for the differences in masses for components which make up the two compounds by using the method described by Bouvier, Lethuillier, and Schmitt.¹³ When the heavier atoms Ce (considered as a nonmagnetic element) and Ru replace the lighter atoms Y and Co, respectively, the measured Debye temperature of 354 K for $Y_3Co_4Ge_{13}$ is reduced to 319 K. This allows one to scale the measured heat capacity of $Y_3Co_4Ge_{13}$ to that of a hypothetical "nonmagnetic" $Ce_3Ru_4Ge_{13}$ compound, which we have designated as " $Y_3Co_4Ge_{13}$." The results are shown in Fig. 7, where we have plotted the measured heat capacity (as C/T) of $Ce_3Ru_4Ge_{13}$ [Fig. 7(a)] and $CeRuGe_3$ [Fig. 7(b)] and that of " $Y_3Co_4Ge_{13}$," and their difference. The difference is essentially constant from 10 to 17 K for the former and to 20 K for the latter ($T^2 = 100$ to 300 and 400 K², respectively) with an average value of 105 ± 5 and 101 ± 8 mJ/(mol Ce) K², respectively, where a mole is based on the $CeRu_{1.33}Ge_{3.33}$ formula unit or on the $CeRuGe_3$ formula unit. The scatter seen in the difference for the two compounds is a reflection of the scatter of the experimental data of $Ce_{4-x}Ru_xGe_{12+x}$ compounds. This analysis assumes that the slight difference in composition for $CeRuGe_3$ has no effect on the heat capacity of " $Y_3Co_4Ge_{13}$." Since the γ value of $Y_3Co_4Ge_{13}$ is 5.7 mJ/(mol Y) K², this value must be added to the C/T values of 105 and 101 giving a value of 111 ± 5 mJ/(mol Ce) K² for the γ of $Ce_3Ru_4Ge_{13}$ and of 107 ± 8 mJ/(mol Ce) K² for $CeRuGe_3$. These values suggest that these compounds are light heavy fermions. But as noted above only two of the cerium atoms are trivalent in the $CeRuGe_3$ unit cell, while the other six are tetravalent, and 1.5 and 4.5, respectively, in the $Ce_3Ru_4Ge_{13}$ unit cell. It is unlikely that the tetravalent cerium or the ruthenium or germanium atoms contribute significantly to the electronic heat capacity, and therefore the large effective masses are primarily due to the

trivalent cerium atoms. This means that the true effective masses of the trivalent cerium atoms are really four times larger (since a mole of cerium in $CeRuGe_3$ consists of two Ce^{3+} and six Ce^{4+} atoms) than indicated from the experimentally derived value, and $\gamma = 428 \pm 32$ mJ/(mol Ce^{3+}) K² for $CeRuGe_3$ making this compound a

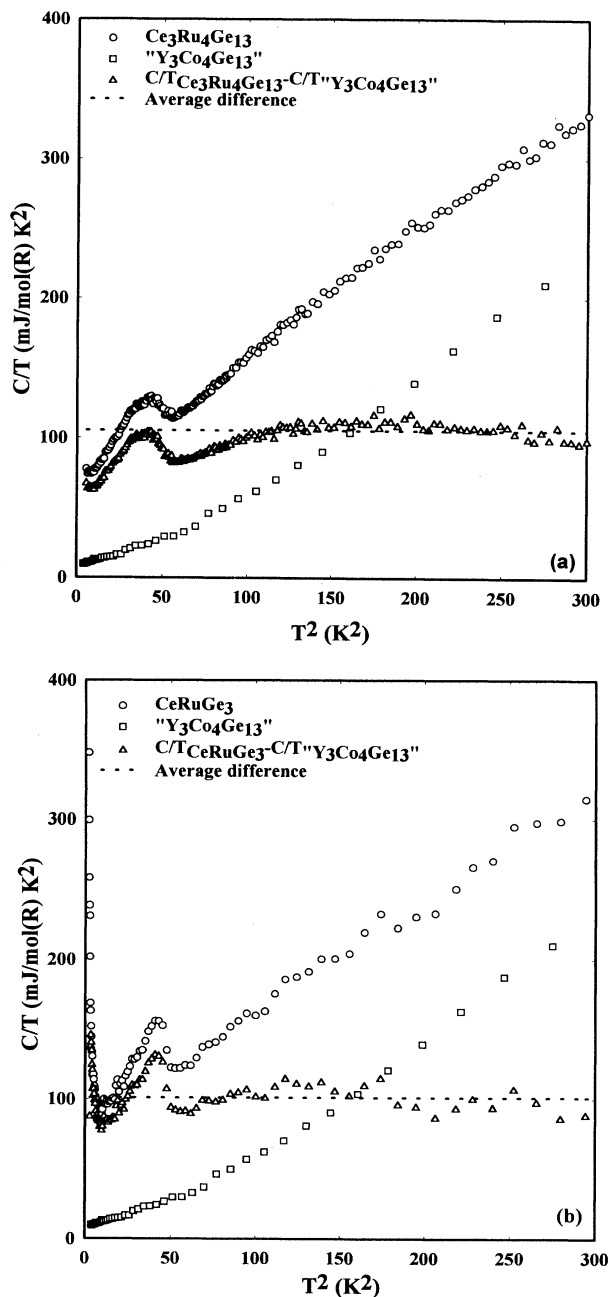


FIG. 7. The heat capacity of (a) $Ce_3Ru_4Ge_{13}$ and (b) $CeRuGe_3$, " $Y_3Co_4Ge_{13}$ " (which is the heat capacity of $Y_3Co_4Ge_{13}$ modified according to the estimated decrease in the Debye temperature from 354 to 319 K, see text), and the difference between the two curves in the form of C/T vs T^2 plots. The short dashed line is the average constant difference between the two C/T vs T^2 plots.

truly heavy-fermion material. For $\text{Ce}_3\text{Ru}_4\text{Ge}_{13}$, γ is also four times larger (here one mole of cerium for $\text{CeRu}_{1.33}\text{Ru}_{3.33}$ consists of 1.5 Ce^{3+} and 4.5 Ce^{4+} atoms) giving an even larger value of $\gamma = 592 \pm 27$ $\text{mJ}/(\text{mol Ce}^{3+})\text{K}^2$. This analysis is consistent with the various Ce-Ce distances in CeRuGe_3 (and also $\text{Ce}_3\text{Ru}_4\text{Ge}_{13}$); see Table II. The Ce1-Ce1 distance is 4.533 Å, while Ce2-Ce2 separation is extremely large at 7.851 Å, and the Ce1-Ce2 distance is 5.068 Å. The Ce1-Ce1 distance and the 428–592 γ values are consistent with the analysis of Meisner *et al.*¹⁴ relating heavy-fermion behavior and f -atom spacings, and fall close the U_2Zn_{17} value on their plot (Fig. 2 in their paper).

The entropy associated with the ~ 6.7 K anomaly is estimated to be ~ 100 $\text{mJ}/(\text{mol Ce})\text{K}$ for $\text{Ce}_3\text{Ru}_4\text{Ge}_{13}$ and ~ 130 $\text{mJ}/(\text{mol Ce})\text{K}$ for CeRuGe_3 . These values are well below (by ~ 100 times) what one would expect for the crystal-field ground-state doublet or quartet [$R \ln 2 = 5.76$ $\text{J}/(\text{mol Ce})\text{K}$ or $R \ln 4 = 11.5$ $\text{J}/(\text{mol Ce})\text{K}$, respectively] if the magnetic ordering is a bulk property of CeRuGe_3 or $\text{Ce}_3\text{Ru}_4\text{Ge}_{13}$. Therefore it is quite possible that a small amount of a magnetic impurity is present in both cerium samples, and this impurity phase orders magnetically at ~ 6.7 K. It is reasonable to assume that the impurity is the binary compound CeGe_2 , since it orders ferromagnetically around 7 K.¹⁵ It was shown by Yashima *et al.*¹⁵ that the entropy associated with ordering in CeGe_2 equals $R \ln 2$, and from this fact we estimate that the amount of CeGe_2 impurity was 1.5 and 2 mol % (1 and 1.3 wt %) for $\text{Ce}_3\text{Ru}_4\text{Ge}_{13}$ and CeRuGe_3 , respectively. A magnetic field of 1 T broadens the ~ 6.7 K heat-capacity bump, and at magnetic fields greater than 2.46 T the magnetic ordering peak is no longer visible, which is consistent with ferromagnetic ordering.

Much more interesting is the behavior of the heat capacity at the lowest temperature (down to ~ 2 K for $\text{Ce}_3\text{Ru}_4\text{Ge}_{13}$ and ~ 1.3 K for CeRuGe_3). Due to the low-temperature limits of our apparatus we were just able to detect the beginning of an upturn at zero magnetic field (inset of Fig. 5) which is clearly more visible in sample No. 2. A magnetic field has a pronounced effect on this low-temperature tail. That is, the magnetic field shifts the tail towards higher temperature, enhancing the total sample's heat capacity at least up to 20 K, and forms a visible broad peak in fields ≥ 5.32 T, which shifts towards high temperature with increasing field. This behavior is typical of a ferromagnet or a spin glass. In order to better understand this low-temperature behavior, ac susceptibility (Fig. 8) and dc magnetization (Fig. 9) measurements have been carried out. The ac susceptibility reveals the presence of a small anomaly around 7 K, which is consistent with all previously described observations and is probably due to the presence of the CeGe_2 impurity. Below ~ 5.5 K the ac susceptibility shows a slight frequency dependence (Fig. 8, open symbols). The ac susceptibility not only exhibits a frequency dependence, but also a field dependence (see inset to Fig. 8). These behaviors suggest that the ground state of CeRuGe_3 is a spin-glass system rather than a ferromagnet. Usually spin-glass systems are characterized by the

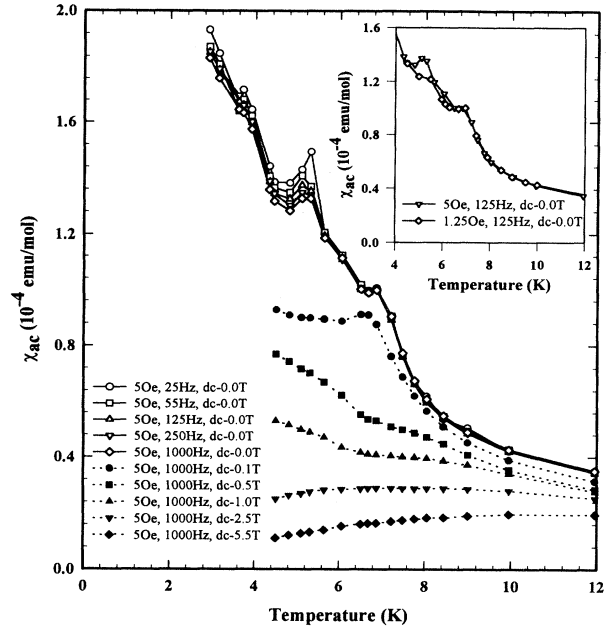


FIG. 8. The ac susceptibility of CeRuGe_3 (sample 2). The ac susceptibility as a function of frequency (open symbols) from ~ 3 to 12 K, and the dependence of the ac susceptibility on the applied dc bias field (solid symbols). The inset shows the effect of the ac field on the susceptibility.

presence of a field- and frequency-dependent maximum of the ac susceptibility. This maximum defines T_f (the freezing temperature), where spins, frustrated by a random distribution of magnetic or nonmagnetic sublattices, freeze randomly. An appropriate heat-capacity max-

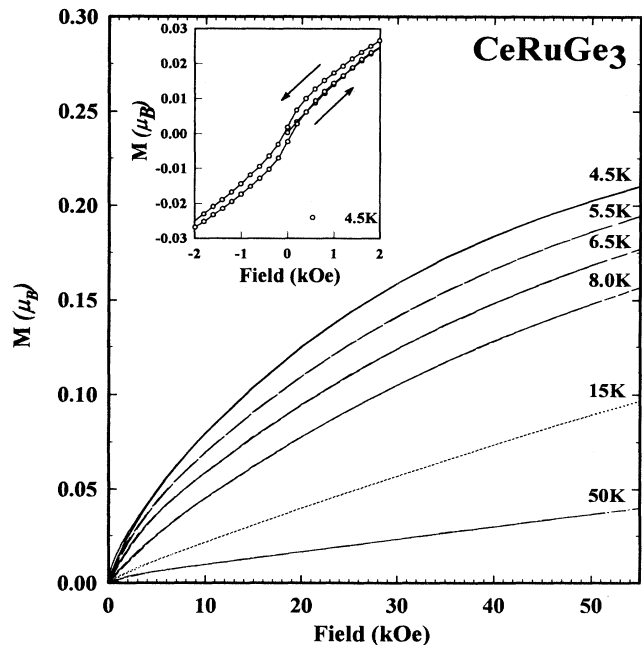


FIG. 9. The magnetization isotherms of CeRuGe_3 (sample 2) with the inset displaying the hysteresis loop at 4.5 K.

imum is usually observed at a somewhat higher temperature than T_f determined from ac susceptibility. As is seen in Fig. 8, the ac susceptibility data of CeRuGe₃ are still rising rapidly at the lowest temperature, just like the heat-capacity tail, suggesting that T_f is less than 2 K. The field- and frequency-dependent maximum around 5.3 K in the ac susceptibility and the absence of a heat-capacity anomaly near this temperature are puzzling but may be due to the unusual structural characteristics of the alloys (see below).

The existence of a spin-glass system in Ce_{4-x}Ru₄Ge_{12+x} may seem to be a surprise especially for the CeRuGe₃ composition. But, if one recalls the details of crystal structure of the samples we are studying, there is disorder in the cerium sublattice (Ce2) as well as in the germanium one. For Ce₃Ru₄Ge₁₃ there is the possibility of an additional disorder, if the germanium and cerium atoms in the 2(*a*) and 6(*d*) sites are randomly occupied. Therefore we believe that the spin-glass transition for the CeRuGe₃ composition is at least a two-step transition: first at $T_f^1 \sim 5.3$ K a positional modulation disorder associated with the cerium atoms in the 2(*a*) sublattices freezes, and then at much lower temperature ($T_f^2 < 1.5$ K) the rest of the cerium spins freeze due to the nonmagnetic atom disorder¹⁶ (NMAD) of the germanium atoms, to form the complete spin-glass system. Based on prior observations¹⁶⁻¹⁹ the NMAD spin-glass T_f occurs slightly below 1 K, and this is consistent with the ac susceptibility and the field dependence of the heat capacity of CeRuGe₃. For the Ce₃Ru₄Ge₁₃ composition the small tail in the heat capacity is consistent with a nonmagnetic atom disorder below 1 K.

Finally, magnetization isotherms (Fig. 9) show that low-temperature ferromagnetism is not likely for the CeRuGe₃ compound, since no trace of saturation is seen up to 5.5 T. A small magnetic hysteresis at $T=4.5$ K, which is shown in the inset, is consistent with the 5.3 K anomaly observed in the ac susceptibility. Therefore the compound CeRuGe₃ can be classified as a heavy-fermion low-temperature spin-glass system where the glassy ground state is caused by a simultaneous disorder in the magnetic and nonmagnetic atom sublattices.

IV. DISCUSSION

A number of cerium intermetallic compounds which contain two inequivalent crystallographic sites are known and have been studied. In most cases the cerium atoms in the different sites exhibit different magnetic and electronic behaviors. In Ce₂Sn₅ the cerium atoms in both sites are essentially trivalent at high temperature,²⁰ but at 4 K one cerium is trivalent and the other is nonmagnetic, exhibiting intermediate-valence behavior.²¹ The cerium atoms in Ce₅Sn₃ are also trivalent at high temperature, but at low temperature one set of cerium atoms orders antiferromagnetically while the second set exhibits heavy-fermion behavior.²² The cerium system Ce_{4-x}Ru₄Ge_{12+x} is different from Ce₂Sn₅ and Ce₅Sn₃ because one of the sites is occupied by trivalent cerium and the other by tetravalent cerium from 4 to 300 K. This

situation is more like that observed in SmRuSn₃ where the Sm atoms in the two sites are trivalent and either divalent or weakly valence fluctuating.²³

Analysis of the heat capacity indicates that this material exhibits heavy-fermion behavior with γ varying from 428 to 592 mJ/(mol Ce³⁺) K² depending on the composition, when taking into account that only the trivalent cerium atoms are involved. Just from these observations, this alloy system is a unique material, but in addition the trivalent cerium atoms and the germanium atoms exhibit crystallographic disorders which are evident from the x-ray and neutron-diffraction intensity data. These disorders account for some anomalous magnetic spin-glass behavior at low temperature, which deviates from that of conventional spin glasses. The latter are usually formed when magnetic ions are diluted in a nonmagnetic lattice, and therefore glassy behaviors arise from magnetic atom disorder (i.e., MAD spin glasses). There are several examples of spin-glass systems which are due to another mechanism of glassy state formation, the so-called nonmagnetic-atom-disorder¹⁶ spin-glass systems: CeCu_{6.5}Al_{6.5},¹⁷ CePd₃B_{0.3},¹⁸ CePtGa₃,¹⁹ and U₂TSi₃ ($T=Fe, Co, Ni, \text{ or } Cu$).²⁴ In these cases it is assumed that the spin system(s) are frozen in a glassy state, because the random distribution of nonmagnetic atoms randomizes the M - M (M is the magnetic ion) exchange interaction, and thus the sublattice of magnetic atoms does not form a long-range magnetically ordered phase. The CeRuGe₃ compound falls between these two groups of spin-glass systems, because it is characterized simultaneously by partial disorder in the magnetic ion sublattice and partial disorder in the nonmagnetic atom sublattice. Similarly to the above it is possible to define the mechanism of glassy state formation as a magnetic/nonmagnetic atom disorder (M/NMAD) spin glass.

We believe that there are several major factors which make possible the spin-glass state in the case of the CeRuGe₃ (Ce₃Ru₄Ge₁₃) compound. The main factor is internal disorder, observed for the cerium sublattice [probably displacement modulation of Ce2 in the 2(*a*) site position]. The second is disorder upon the nonmagnetic atom sublattice: germanium in the 24(*k*) position. The influence of this, probably a 2D or 3D modulated sublattice, is less important than the first factor, but it definitely contributes to magnetic ion sublattice frustration too. The case for CeRuGe₃ and Ce₃Ru₄Ge₁₃ is not typical for most of the known NMAD spin-glass systems, because in none of the four above examples is the disorder caused by a modulation-type disorder. All of the known NMAD spin-glass systems have a glassy origin (i.e., randomized exchange interaction) caused by a simple statistical distribution of different nonmagnetic atoms in the same sublattice: in CeCu_{6.5}Al_{6.5},¹⁷ the Cu and Al atoms are located statistically in the same sublattice; in CePd₃B_{0.3},¹⁸ the boron atoms and vacancies are randomly distributed in the boron sublattice; in CePtGa₃,¹⁹ the Pt and Ga atoms are statistically mixed in the same sublattice; and in U₂TSi₃ ($T=Fe, Co, Ni, \text{ or } Cu$),²⁴ the transition-metal and Si atoms are again mixed statistically in the same sublattice of nonmagnetic atoms. In all of the above cases, except

the U_2TSi_3 compounds, the magnetic atoms (Ce) have a stable valence with an effective magnetic moment close to the magnetic moment of the free Ce^{3+} ion. Only in the U_2TSi_3 phases does the U magnetic atom display a mixed-valent state in addition to the statistical nonmagnetic atom arrangement.

ACKNOWLEDGMENTS

The Ames Laboratory is operated by the U.S. Department of Energy by Iowa State University under Contract No. W-7405-ENG-82. This work was supported by the Office of Basic Energy Sciences.

- ¹*Topics in Superconductivity in Ternary Compounds*, edited by M. B. Maple and F. Fisher (Springer-Verlag, Berlin, 1982), Vol. 2.
- ²J. P. Remeika, G. P. Espinosa, A. S. Cooper, H. Barz, J. M. Rowell, D. B. McWhan, J. M. Vandenberg, D. E. Moncton, Z. Fisk, L. D. Wolf, H. C. Hamaker, M. B. Maple, G. Shirane, and W. Thomlinson, *Solid State Commun.* **34**, 923 (1980).
- ³C. U. Segre, H. F. Braun, and K. Yvon, in *Ternary Superconductors*, edited by G. K. Shenoy, B. D. Dunlap, and F. Y. Fradin (North-Holland, Amsterdam, 1981), p. 243.
- ⁴J. L. Hodeau, M. Marezio, J. P. Remeika, and C. H. Chen, *Solid State Commun.* **42**, 97 (1982).
- ⁵B. Eisenmann and H. Schäfer, *J. Less-Common Met.* **123**, 89 (1986).
- ⁶V. A. Bruskov, V. K. Pecharsky, and O. I. Bodak, *Izv. Akad. Nauk. SSSR Neorg. Mater.* **22**, 1471 (1986) [*Inorg. Mater.* **22**, 1289 (1986)].
- ⁷S. Ramakrishnan, S. Sundaram, R. S. Pandit, and Girish Chandra, *J. Phys. E* **42**, 1373 (1985).
- ⁸K. Ikeda, K. A. Gschneidner, Jr., B. J. Beaudry, and U. Atzmony, *Phys. Rev. B* **25**, 4604 (1982).
- ⁹L. G. Akselrud, Yu. N. Grin, P. Yu. Zavalij, V. K. Pecharsky, and V. S. Fundamensky, in *XIIth European Crystallographic Meeting, Collected Abstracts*, edited by B. K. Vainshtein and A. M. Prokhorov (USSR Academy of Sciences, Moscow, 1989), Vol. 3, p. 155.
- ¹⁰V. K. Pecharsky, K. A. Gschneidner, Jr., and L. L. Miller, *Phys. Rev. B* **43**, 10 906 (1991).
- ¹¹D. C. Koskenmaki and K. A. Gschneidner, Jr., in *Handbook on the Physics and Chemistry of Rare Earths*, edited by K. A. Gschneidner, Jr., and L. Eyring (North-Holland, Amsterdam, 1978), Vol. 1, p. 337.
- ¹²G. R. Stewart, *Rev. Mod. Phys.* **56**, 755 (1984).
- ¹³M. Bouvier, P. Lethuillier, and D. Schmitt, *Phys. Rev. B* **43**, 13 137 (1991).
- ¹⁴G. P. Meisner, A. L. Giorgi, A. C. Lawson, G. R. Stewart, J. O. Willis, M. S. Wire, and J. L. Smith, *Phys. Rev. Lett.* **53**, 1829 (1984).
- ¹⁵H. Yashima, T. Satoh, H. Mori, D. Watanabe, and T. Ohtsuka, *Solid State Commun.* **41**, 1 (1982).
- ¹⁶K. A. Gschneidner, Jr., J. Tang, S. K. Dhar, and A. Goldman, *Physica B* **163**, 507 (1990).
- ¹⁷U. Rauchschwalbe, U. Gottwick, U. Ahlheim, H. M. Mayer, and F. Steglich, *J. Less-Common Met.* **111**, 265 (1985).
- ¹⁸S. K. Dhar, K. A. Gschneidner, Jr., C. D. Bredl, and F. Steglich, *Phys. Rev. B* **39**, 2439 (1989).
- ¹⁹J. Tang, K. A. Gschneidner, Jr., R. Caspary, and F. Steglich, *Physica B* **163**, 151 (1989).
- ²⁰S. K. Dhar, K. A. Gschneidner, Jr., and O. D. McMasters, *Phys. Rev. B* **35**, 3291 (1987).
- ²¹J. X. Boucherle, F. Givord, F. Lapierre, P. Lejay, J. Peyrard, J. Odin, J. Schweizer, and A. Stunault, in *Theoretical and Experimental Aspects of Valence Fluctuations and Heavy Fermions*, edited by L. C. Gupta and S. K. Malik (Plenum, New York, 1987), p. 485.
- ²²J. M. Lawrence, M. F. Hundley, J. D. Thompson, G. H. Kwei, and Z. Fisk, *Phys. Rev. B* **43**, 11 057 (1991).
- ²³C. Godart, C. Mazumdar, S. K. Dhar, R. Nagarajan, L. C. Gupta, B. D. Padalia, and R. Vijayaraghavan, *Phys. Rev. B* **48**, 16 402 (1993).
- ²⁴D. Kaczorowski and H. Noël, *J. Phys. Condens. Matter* **5**, 9185 (1993).